Atmospheric Environment 167 (2017) 323–334

Contents lists available at ScienceDirect

Atmospheric Environment

journal homepage: www.elsevier.com/locate/atmosenv

Global budget of tropospheric ozone: Evaluating recent model advances with satellite (OMI), aircraft (IAGOS), and ozonesonde observations

Lu Hu [a, b, *], Daniel J. Jacob [a, c], Xiong Liu [d], Yi Zhang [e, 1], Lin Zhang [e], Patrick S. Kim [a], Melissa P. Sulprizio [a], Robert M. Yantosca [a]

[a] School of Engineering and Applied Sciences, Harvard University, Cambridge, MA, USA
[b] Department of Chemistry and Biochemistry, University of Montana, Missoula, MT, USA
[c] Department of Earth and Planetary Science, Harvard University, Cambridge, MA, USA
[d] Atomic and Molecular Physics Division, Harvard Smithsonian Center for Astrophysics, Cambridge, MA, USA
[e] Department of Atmospheric and Oceanic Sciences, School of Physics, Peking University, Beijing, China

HIGHLIGHTS

- GEOS-Chem updates over past decade have led to more active model ozone chemistry.
- V10-01 improves tropospheric ozone simulation relative to earlier model versions.
- A prominent flaw occurs at high northern latitudes, likely due to insufficient STE.
- GEOS-Chem ozone burden, production, & lifetime are on high side of other models.
- OMI data maintained persistent high quality and no significant drift over 2006–2013.

ARTICLE INFO

Article history:
Received 7 March 2017
Received in revised form
10 August 2017
Accepted 14 August 2017
Available online 16 August 2017

Keywords:
Tropospheric ozone
Budget
Chemical transport model
Satellite
Ozonesonde
Aircraft

ABSTRACT

The global budget of tropospheric ozone is governed by a complicated ensemble of coupled chemical and dynamical processes. Simulation of tropospheric ozone has been a major focus of the GEOS-Chem chemical transport model (CTM) over the past 20 years, and many developments over the years have affected the model representation of the ozone budget. Here we conduct a comprehensive evaluation of the standard version of GEOS-Chem (v10-01) with ozone observations from ozonesondes, the OMI satellite instrument, and MOZAIC-IAGOS commercial aircraft for 2012–2013. Global validation of the OMI 700-400 hPa data with ozonesondes shows that OMI maintained persistent high quality and no significant drift over the 2006–2013 period. GEOS-Chem shows no significant seasonal or latitudinal bias relative to OMI and strong correlations in all seasons on the $2^\circ \times 2.5^\circ$ horizontal scale ($r = 0.88$–0.95), improving on previous model versions. The most pronounced model bias revealed by ozonesondes and MOZAIC-IAGOS is at high northern latitudes in winter-spring where the model is 10–20 ppbv too low. This appears to be due to insufficient stratosphere-troposphere exchange (STE). Model updates to lightning NO_x, Asian anthropogenic emissions, bromine chemistry, isoprene chemistry, and meteorological fields over the past decade have overall led to gradual increase in the simulated global tropospheric ozone burden and more active ozone production and loss. From simulations with different versions of GEOS meteorological fields we find that tropospheric ozone in GEOS-Chem v10-01 has a global production rate of 4960–5530 Tg a^{-1}, lifetime of 20.9–24.2 days, burden of 345–357 Tg, and STE of 325–492 Tg a^{-1}. Change in the intensity of tropical deep convection between these different meteorological fields is a major factor driving differences in the ozone budget.

1. Introduction

Tropospheric ozone (O_3) is an important greenhouse gas, a

* Corresponding author.
E-mail address: lu.hu@mso.umt.edu (L. Hu).
[1] Now at Atmospheric and Oceanic Sciences Program, Princeton University, Princeton, NJ, USA.

http://dx.doi.org/10.1016/j.atmosenv.2017.08.036
1352-2310/

surface pollutant, and the primary precursor of the hydroxyl radical (the main atmospheric oxidant). Understanding the factors controlling tropospheric ozone is a central problem in atmospheric chemistry. Ozone is transported to the troposphere from the stratosphere, and is also produced within the troposphere by photo-oxidation of volatile organic compounds (VOCs) and carbon monoxide (CO) in the presence of nitrogen oxides ($NO_x \equiv NO + NO_2$). These precursors have both anthropogenic and natural sources, and lifetimes ranging from minutes to years. Ozone has a lifetime of a few weeks and is eventually removed by photochemical loss and dry deposition. Here we use an ensemble of satellite, aircraft, and sonde measurements to test our understanding of the tropospheric ozone budget as simulated by the GEOS-Chem global 3-D chemical transport model (CTM), and we examine the role of major new GEOS-Chem developments in affecting the ozone simulation.

Simulation of global tropospheric ozone has long been a target of atmospheric chemistry models. A large database of observations is available from the ozonesonde network (Logan, 1999; Thompson et al., 2007). Observations are also made from commercial aircraft (Brenninkmeijer et al., 2007; Volz-Thomas et al., 2009; Nédélec et al., 2015). Global mapping of tropospheric ozone from space began in the 1980s (Fishman et al., 1986; Fishman and Larsen, 1987), and has since expanded with direct retrievals in both the infrared (IR) (Worden et al., 2007) and the ultraviolet (UV) (Liu et al., 2005, 2006). Current state-of-science CTMs typically show a successful simulation of global tropospheric ozone including its large-scale gradients and seasonal variations (Stevenson et al., 2006; Fiore et al., 2009; Young et al., 2013). However, the global ozone production and loss rates can vary by a factor of 2 or more between models (Wild, 2007; Wu et al., 2007). Models are also unable to reproduce observed centurial and multi-decadal trends (Mickley et al., 2001; Parrish et al., 2014).

Simulation of global tropospheric ozone has been a major driver in the development of the GEOS-Chem CTM, starting from the original model described by Bey et al. (2001). Wu et al. (2007) showed the evolution of the global tropospheric ozone budget in successive GEOS-Chem versions pre-2006 and Fig. 1 shows the effect of more recent developments. These include in particular updating Asian anthropogenic emissions, improving lightning NO_x emissions by using satellite data for individual years (Murray et al., 2012), improving biogenic VOC chemistry (Paulot et al., 2009a, 2009b), implementing tropospheric bromine chemistry (Parrella et al., 2012), and using newer-generation assimilated meteorological data. These changes have overall led to a gradual upward creep in the global tropospheric ozone burden and production rate.

The last global evaluation of the GEOS-Chem simulation of tropospheric ozone was presented by Zhang et al. (2010) using v8-01-04 of the model released in March 2009. That work used worldwide ozonesonde data as well as satellite observations from the TES and OMI instruments. It found that GEOS-Chem systemically underestimated ozone in the tropics and overestimated ozone in the northern subtropics and southern mid-latitudes. Here we revisit the global evaluation of the GEOS-Chem tropospheric ozone simulation using ozonesonde, satellite, and aircraft data, to examine in particular if the flaws previously identified by Zhang et al. (2010) have been corrected and if new flaws have developed. We focus on the global ozone distribution. Other recent GEOS-Chem studies have examined the capability of the model to simulate ozone precursors for individual regions (Wang et al., 2011; Marais et al., 2012; Hu et al., 2015; Jiang et al., 2015; Johnson et al., 2016; Sofen et al., 2016; Yan et al., 2016) and the correlation of ozone with its precursors regionally and globally (Kim et al., 2013; Travis et al., 2016).

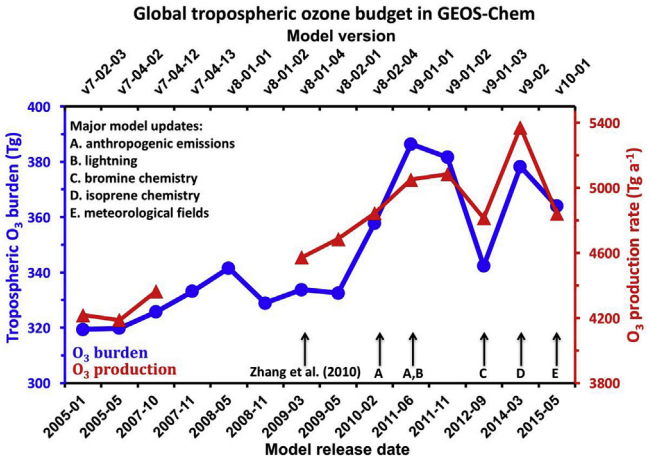

Fig. 1. Evolution of the annual mean global tropospheric ozone burden and production rate in successive versions of the GEOS-Chem model. Data are from benchmark simulations conducted when new versions of the model are released. All benchmark simulations are done for the same meteorological and emission year of 2005, except for the first two (2001 for v7-02-03 and v7-04-02) and the last one (2013 for v10-01). All benchmark simulations are conducted at 4° × 5° horizontal resolution with 12 months of spin-up. Major model developments and the version previously evaluated by Zhang et al. (2010) are identified with vertical arrows. Ozone production rate is for the odd oxygen (O_x) chemical family to account for fast cycling between ozone and short-lived reservoirs. Documentation for all versions and benchmarking procedure are at http://www.geos-chem.org. A similar figure for pre-2006 versions of the GEOS-Chem ozone budget is shown in Wu et al. (2007).

2. GEOS-chem chemical transport model

2.1. General description

We use GEOS-Chem v10-01 (http://www.geos-chem.org) driven by assimilated meteorological data from the Goddard Earth Observing System (GEOS) of the NASA Global Modeling and Assimilation Office (GMAO). Operational GEOS data are produced by GMAO with a grid resolution of 0.25° × 0.3125° (latitude by longitude) and 72 vertical levels extending up to 0.01 hPa. They are archived every 3 h (1 h for surface data). Here we conduct GEOS-Chem simulations at 2° × 2.5° resolution for 2011–2013 by averaging the native-resolution meteorological data, with time steps of 15 min for transport and 30 min for chemistry (Philip et al., 2016). We use 12 months for initialization and report results for June 2012–May 2013. This time period is chosen because of the overlap of two versions of operational GEOS-5 meteorological data produced by GMAO, allowing us to examine the sensitivity to meteorology. Hereinafter we refer to the latest version of meteorological data (GEOS-5.7.2 and later versions) as GEOS-5 Forward-Processing or GEOS-FP, and to the previous version (GEOS-5.2.0) as GEOS-5. We will also show results from a sensitivity simulation with older-generation GEOS-4 meteorological fields available through 2006.

Emissions in GEOS-Chem are computed by the Harvard-NASA Emission Component (HEMCO) (Keller et al., 2014), which combines and regrids ensembles of user-selected regional and global emission inventories. Global emissions used here are given in Table 1. The model includes detailed HO_x-NO_x-VOC-ozone-BrO_x-aerosol tropospheric chemistry with JPL and IUPAC recommendations for chemical kinetics (Sander et al., 2011; IUPAC, 2013). BrO_x chemistry is from Parrella et al. (2012) and isoprene oxidation chemistry is from Mao et al. (2013). Photolysis frequencies are calculated with the Fast-JX scheme (Bian and Prather, 2002), as implemented in GEOS-Chem by Mao et al. (2010) and Eastham et al. (2014). Stratospheric chemistry is represented using the Linoz

algorithm of McLinden et al. (2000) for ozone and monthly mean production and loss rate constants for other stratospheric gases (Murray et al., 2012). Dry deposition in GEOS-Chem is calculated using a resistance-in-series model based on Wesely (1989) and implemented by Wang et al. (1998), with recent updates for reactive uptake by vegetation (Karl et al., 2010).

2.2. Recent model developments affecting ozone

Fig. 1 shows the evolution of the global tropospheric ozone budget through the recent 10-year benchmark history of GEOS-Chem standard model versions. Changes mainly reflect model advances, not the actual atmosphere, though the benchmark has been updated to year 2013 since version v10-01. There is an increasing trend in the tropospheric ozone burden. The ozone burden in GEOS-Chem v10-01 benchmark (363 Tg; conducted at 4° × 5° resolution) is at the high end of other models (337 ± 23 Tg ACCMIP and 344 ± 39 Tg ACCENT ensemble model mean (Stevenson et al., 2006; Young et al., 2013)). However, we will show that this value is not too high relative to observations.

Also shown in Fig. 1 is the trend in the ozone production rate (as odd oxygen), which similarly shows a general increase. A review of global models by Wu et al. (2007) previously found a large increase in global annual mean ozone production rates from pre-2000 models (3400 ± 800 Tg a^{-1}) to post-2000 models (4600 ± 600 Tg a^{-1}) due to higher NO_x emissions, better representation of VOC chemistry, and lower (more realistic) stratospheric influx. Here we find a continued growth in the ozone production rate over the past decade of GEOS-Chem development, indicative of even more active ozone chemistry. Several major new developments in GEOS-Chem have driven these changes.

Anthropogenic emissions. NO_x and CO emissions in East Asia were updated in GEOS-Chem v9-01-01 (Li et al., 2014). This increased the global NO_x emission from 21 to 28 Tg N a^{-1} and CO emission from 340 to 500 Tg a^{-1}, and increased the global tropospheric ozone burden by 5% and ozone production rate by 7%.

Lightning. Lightning NO_x emission (LNO_x) in GEOS-Chem is constrained by satellite lightning flash data in a way that preserves the coupling of NO_x release with deep convective transport (Sauvage et al., 2007; Murray et al., 2012). A new LNO_x representation from Murray et al. (2012) to better couple lightning and deep convection on regional scales was introduced in GEOS-Chem v9-01-01 but had little impact on the global ozone budget. The global LNO_x has remained at ~6 Tg N a^{-1} in all versions (Martin et al., 2007; Sauvage et al., 2007). The inferred NO_x yield per flash is 500 mol N at mid-latitudes and 260 mol N in the tropics, consistent with observations (Schumann and Huntrieser, 2007; Ott et al., 2010).

Bromine. Tropospheric bromine chemistry was implemented into GEOS-Chem v9-01-03 by Parrella et al. (2012). This decreased the global tropospheric ozone burden by 6.5%, reflecting decrease in both ozone production (4%) and the lifetime of ozone against chemical loss (3%). The decrease in production was due to the added NO_x sink from $BrNO_3$ formation and hydrolysis to HNO_3. The increase in ozone loss was due to bromine-catalyzed cycles, mainly involving HOBr. The largest effect was in the northern extratropics in spring where ozone decreased by more than 8 ppb (Parrella et al., 2012).

Isoprene. An updated isoprene oxidation mechanism based on recent laboratory work (Paulot et al., 2009a, 2009b; Crounse et al., 2011) was implemented in GEOS-Chem v9-02 by Mao et al. (2013). This includes in particular a decreased role of isoprene nitrates as sink for NO_x. The yield of isoprene nitrates from the reaction of isoprene peroxy radicals with NO decreased from 18% to 12%, and 55% of these nitrates returned NO_x through photolysis whereas they were previously terminal sinks of NO_x. Other isoprene chemistry updates affected low-NO_x conditions. The updated isoprene chemistry increased the global tropospheric ozone burden and production rate by 10% and 15% respectively.

Meteorology. NASA GMAO began producing operationally the GEOS-FP meteorological data with 0.25° × 0.3125° resolution in May 2012 (Molod et al., 2015). GEOS-Chem simulations can now be conducted with GEOS-FP or with older/coarser GMAO meteorological data (GEOS-4, GEOS-5, MERRA, MERRA-2) but GEOS-FP is the default. Switching from GEOS-5 to GEOS-FP meteorology decreased the tropospheric ozone burden and production rate by 4% and 10% respectively. GEOS-FP has less subgrid convection than the older GMAO products because part of the convection is resolved on the grid scale as vertical advection (Yu et al., 2017). Surface temperatures in the tropics are also lower, leading to 30% lower global biogenic VOC and soil NO_x emissions (Table 1).

Table 1
GEOS-Chem global annual emissions for 2013.

Species	Emission	References and notes
NO_x (Tg N a^{-1})		
Fossil fuel	28.1	EDGARv4.2 (Olivier and Berdowski, 2001) [a]
Soil [b]	7.9	Hudman et al. (2012)
Lightning	6.0	Murray et al. (2012)
Open fires	3.7	GFED4 (Giglio et al., 2013)
Fertilizer	1.8	Hudman et al. (2012)
Aircraft	0.8	AEIC (Stettler et al., 2011)
Biofuel	0.7	Yevich and Logan (2003)
Non-methane VOCs (Tg C a^{-1}) [c]		
Isoprene [b]	418	MEGANv2.1(Guenther et al., 2012)
Other biogenic VOCs [b]	350	MEGANv2.1 (Guenther et al., 2012)
Fossil fuel	48.8	RETRO (Schultz et al., 2007) [a]
Open fires	14.3	GFED4 (Giglio et al., 2013)
CO (Tg a^{-1})		
Fossil fuel	482	EDGARv4.2 (Olivier and Berdowski, 2001) [a]
Open fires	280	GFED4 (Giglio et al., 2013)
Biofuel	59	Yevich and Logan (2003)

[a] Superseded with regional inventories for East Asia (MIX; Li et al. (2014)); Europe (EMEP; Auvray and Bey (2005)); Canada (CAC; http://www.ec.gc.ca/inrp-npri/); Mexico (BRAVO; Kuhns et al. (2005)); U.S. (US EPA NEI11; (http://www.epa.gov/ttn/chief/net/2008report.pdf). We use the most recent year available for MIX (2010) and EMEP (2012). CAC and BRAVO emissions are scaled to 2010 (van Donkelaar et al., 2008) and US NEI emissions are scaled to 2013 (https://www3.epa.gov/airtrends/).

[b] Biogenic emissions depend on meteorological data set used and are given here for GEOS-FP. With GEOS-5 these values are 9.6 Tg N a^{-1} for soil NO_x, 574 Tg C a^{-1} for isoprene, and 420 Tg C a^{-1} for other biogenic VOCs. With GEOS-4 the corresponding values are 12.3, 548, and 404. Interannual variability for a given meteorological data set is <5%.

[c] Emitted non-methane VOCs in GEOS-Chem include isoprene, ≥C_4 alkanes, ≥C_4 ketones, propane, acetone, ≥C_3 alkenes, ethane, ethene, acetaldehyde, formaldehyde. The model uses fixed tropospheric methane concentrations of 1761–1893 ppb dependent on latitude (NOAA ESRL data), and fixed methanol concentrations in the boundary layer and free troposphere (Heikes et al., 2002).

3. Observational datasets for model evaluation

3.1. Sonde, aircraft, and OMI satellite observations

We evaluate our 2012–2013 simulation with ozone observations from (a) the worldwide network of ozonesondes, (b) the MOZAIC-IAGOS commercial aircraft program, and (c) the OMI (Ozone Monitoring Instrument) satellite instrument. Ozonesonde locations and MOZAIC-IAGOS flight tracks are shown in Fig. 2.

Ozonesonde observations are taken from the World Ozone and Ultraviolet Data Center (WOUDC, http://www.woudc.org) and the NOAA Earth System Research Laboratory - Global Monitoring Division (NOAA ESRL-GMD, ftp://ftp.cmdl.noaa.gov/ozww/Ozonesonde/). We only use data from Electrochemical Concentration Cell (ECC) and Carbon Iodine (CI) sonde types and do not apply WOUDC-suggested correction factors as their effect is insignificant

(Tanimoto et al., 2015). We have 1895 ~weekly profiles from 41 stations available from June 2012 to May 2013 (Table S1). These stations are grouped into coherent regions (Fig. 2) following Tilmes et al. (2012) to improve statistics.

MOZAIC-IAGOS aircraft observations for 2012–2013 (Thouret et al., 1998; Nedelec et al., 2003; Volz-Thomas et al., 2009) are extracted from http://iagos.fr/extract and we sample the model outputs along flight tracks. We focus on the data at cruising altitudes (300-200 hPa). Recent studies find good agreement between ozonesonde and MOZAIC-IAGOS observations (Tilmes et al., 2012; Tanimoto et al., 2015).

The OMI instrument is onboard the NASA Aura satellite with Equator crossing time of ~13:45 LT (local time). Here we use the OMI PROFOZ ozone profile (partial column) retrievals developed by Liu X et al. (2010) with minor updates described by Kim et al. (2013). The vertical profiles have ~1 piece of information in the troposphere with maximum weight in the middle troposphere at 700-400 hPa. We grid the OMI data to 2° × 2.5° resolution and use the 700-400 hPa partial column data for model evaluation. We exclude data poleward of 60° where instrument sensitivity is very weak, and also filter out retrievals with effective cloud fraction greater than 30%, total degrees of freedom less than 0.5, and root mean square fitting residuals greater than 3% of the measurement error (Kim et al., 2013).

3.2. OMI validation with ozonesonde data

Zhang et al. (2010) demonstrated general consistency of the OMI tropospheric ozone data for 2006 with concurrent data from the TES thermal IR instrument aboard Aura and with ozonesondes. The OMI bias relative to ozonesondes was 2.8 ± 6.6 ppbv and differences with TES were generally less than 10 ppbv. Starting in 2009 the OMI instrument began to experience a "row anomaly" error (partial blockage of the field of view). Here we examine the implications for the OMI tropospheric ozone retrieval by comparing the 2011–2013 and 2008 OMI data at 700-400 hPa to collocated sonde data. We apply the OMI averaging kernel smoothing to the ozonesonde data following Zhang et al. (2010), and require coincident measurements within 1.25° longitude, 1° latitude, and 10 h. This results in 1311 coincidences for 2011–2013 and 889 for 2008.

Statistics summarized in Fig. 3 show that OMI ozone data quality degraded only slightly over the 2006–2013 period. The global mean bias relative to the sondes is 3.6 ± 8.5 ppbv for 2011–2013, as compared to 2.7 ± 6.6 ppbv for 2008 and 2.8 ± 6.6 ppbv for 2006 reported by Zhang et al. (2010). The bias is similar at northern mid-latitudes and in the tropics, and lower at southern mid-latitudes. The results here are generally consistent with independent OMI validation against ozonesondes (Huang et al., 2017). The larger

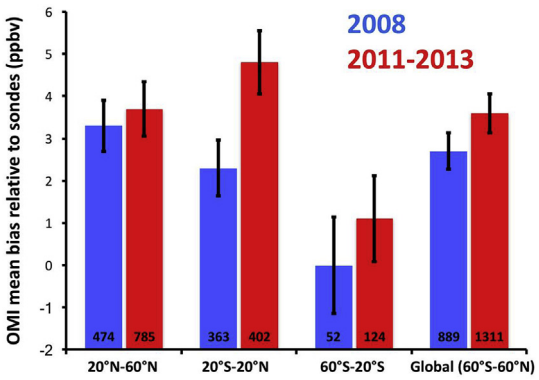

Fig. 3. Mean OMI ozone biases relative to coincident ozonesondes observations for 2008 and 2011–2013. Error bars show the 95% confidence interval for the OMI mean bias. The number of coincidences is given.

standard deviation in 2011–2013 is due to the increase of retrieval noise and the impacts of OMI row anomaly.

Fig. 4 shows seasonal scatterplots of coincident OMI and ozonesonde measurements at 700-400 hPa for 2011–2013. The OMI ozone biases are consistent across sites and have little seasonal variation. Thus the OMI data can be corrected for a mean global bias (3.6 ppbv) and then used for model evaluation to provide full spatial coverage. An exception is for high northern latitudes (>45°N) in winter-spring where OMI has large biases (Fig. 4). We exclude these data from further analysis.

4. Model evaluation

4.1. Evaluation with OMI mid-tropospheric data

Fig. 5 shows the global distribution of tropospheric ozone at 700-400 hPa observed by OMI and simulated by GEOS-Chem (sampled along the OMI tracks) for four seasons in 2012/2013. OMI data have been reprocessed with a single fixed a priori profile (annual mean profile for 30°S-30°N from McPeters et al. (2007)) so that all patterns reflect the measurements themselves. We also correct OMI data for their global mean bias relative to ozonesondes as discussed above. Well-known major features of the ozone distribution are consistent between observations and the model. Concentrations are elevated during MAM and JJA at northern mid-latitudes, reflecting strong stratosphere-troposphere exchange (STE) and high photochemical production. Concentrations are enhanced downwind of South America and Africa during SON because of biomass burning. Ozone is low over the Equatorial Pacific because of fast photochemical loss but is relatively high over the South Atlantic because of subsidence.

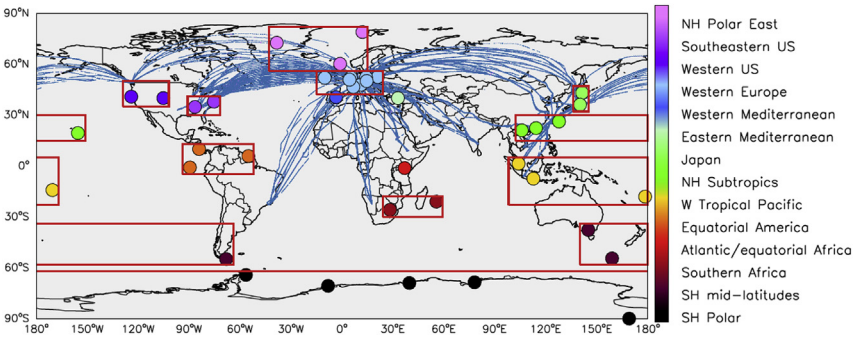

Fig. 2. Ozonesonde (circles) and MOZAIC-IAGOS aircraft (blue lines) data in June 2012–May 2013 used for model evaluation. Red boxes group sites by coherent regions (Tilmes et al., 2012) as analyzed in the text. (For interpretation of the references to colour in this figure legend, the reader is referred to the web version of this article.)

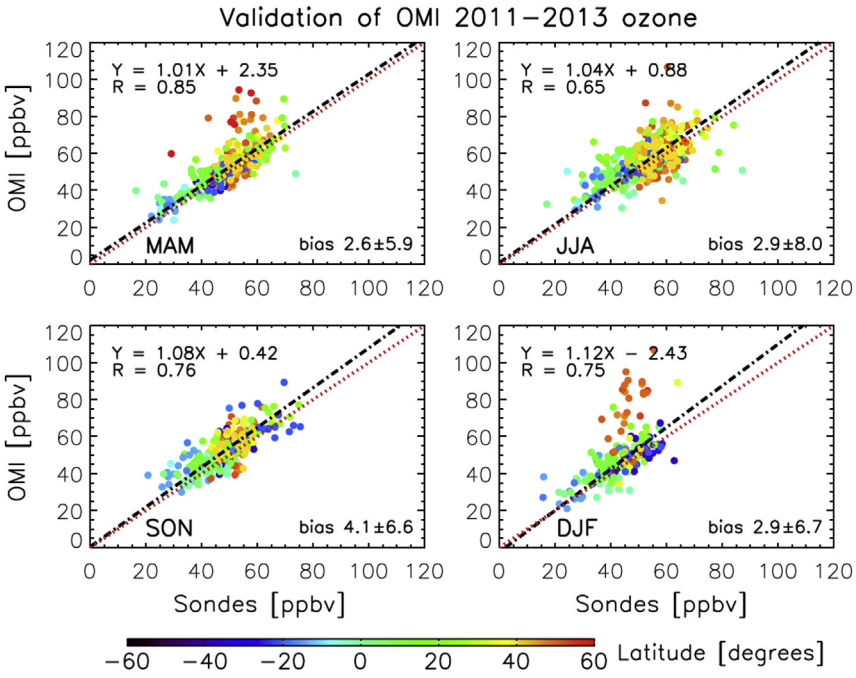

Fig. 4. OMI ozone retrievals at 700-400 hPa compared to ozonesonde observations for four seasons of 2011–2013. Ozonesonde observations are smoothed by the OMI averaging kernels. Each point represents the coincident measurements at a sonde launch site. Black dashed lines show the best fit (reduced major axis regression), with regression parameters given inset. OMI winter (DJF) and spring (MAM), measurements north of 45°N have large errors and are not included in the regression fit. Numbers on the bottom right of each panel are the global mean OMI bias ± standard deviation. The 1:1 line is shown in red. (For interpretation of the references to colour in this figure legend, the reader is referred to the web version of this article.)

GEOS-Chem shows no significant global bias relative to OMI. Seasonal biases are less than 1 ppbv and the global annual mean bias is 0.6 ± 2.3 ppbv. Comparison to OMI on the 2° × 2.5° grid scale (Fig. 6) shows high spatial correlation for different seasons (R = 0.88–0.95). There are patterns of regional biases in Fig. 5 though these tend to be less than 10 ppbv. In particular, there is

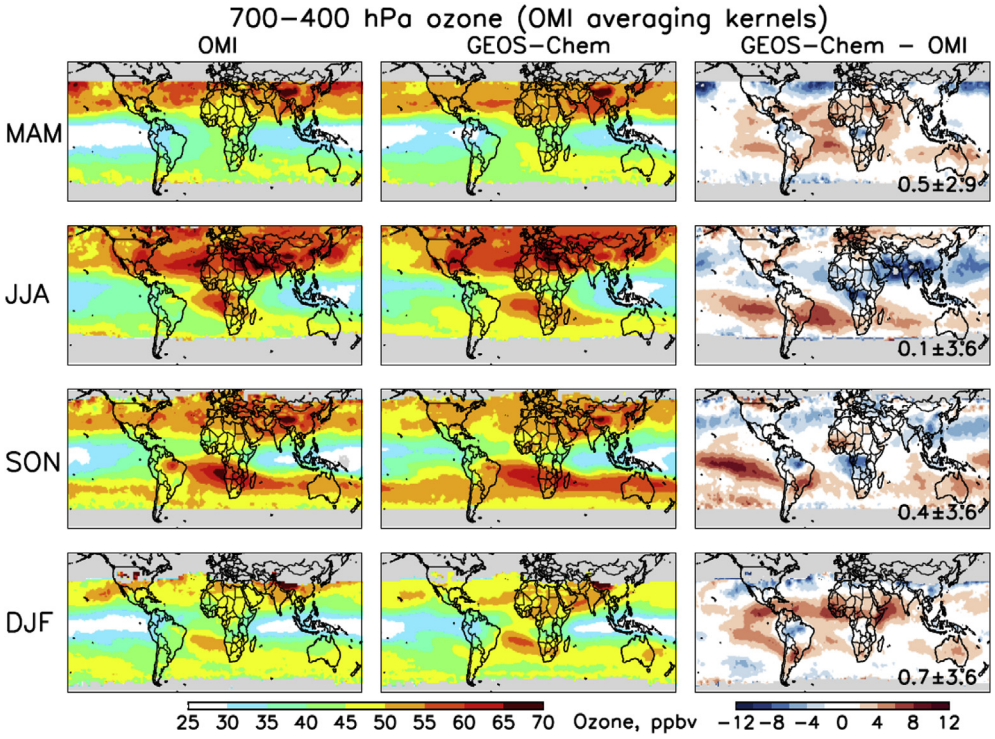

Fig. 5. Mid-tropospheric ozone distribution at 700-400 hPa from OMI (left column) and simulated by GEOS-Chem (middle column) for four seasons in 2012/2013. Also shown is the difference between GEOS-Chem and OMI (right column). OMI measurements use a single fixed a priori as described in the text, and have been corrected for a global mean positive bias of 3.6 ppbv. GEOS-Chem is sampled along the OMI tracks and the simulated ozone mixing ratios are smoothed by the OMI averaging kernels. Numbers in the right column are the mean model bias ± standard deviation. Gray shading indicates regions where OMI data are unreliable and not used (poleward of 45° in winter-spring and poleward of 60° year-round).

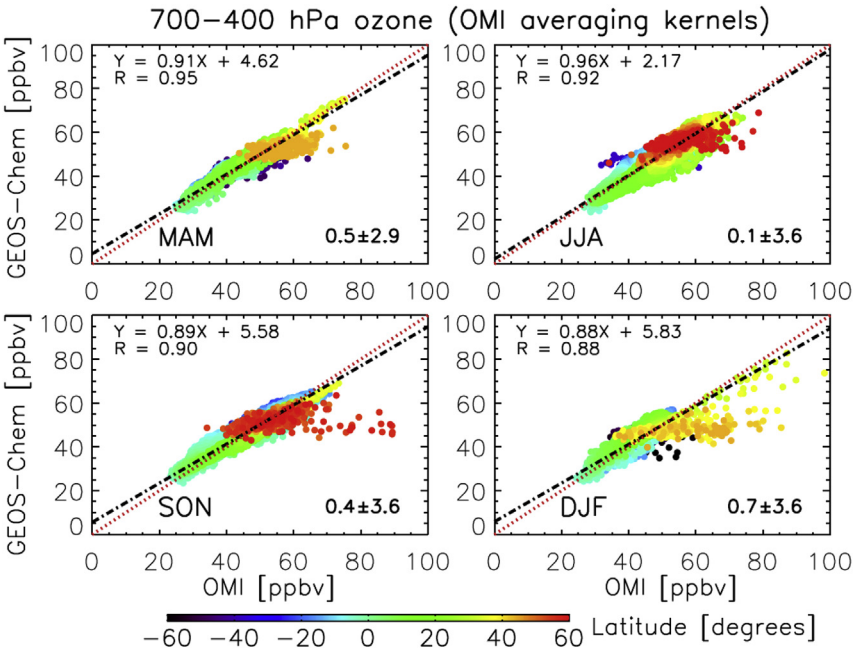

Fig. 6. Comparison of GEOS-Chem ozone with OMI measurements at 700-400 hPa for four seasons in June 2012–May 2013, colored by the latitude of the observations. Each point represents the seasonal mean for a 2° × 2.5° grid cell. Black dashed lines show the best fit (reduced major axis regression) with regression parameters given inset. Numbers on the bottom right are the global mean model bias ± standard deviation. The 1:1 line is shown in red. (For interpretation of the references to colour in this figure legend, the reader is referred to the web version of this article.)

indication of an underestimate at northern mid-latitudes.

We investigate further the latitudinal structure of the model bias in Fig. 7. The major latitudinal features observed by OMI are well reproduced, including the sharp tropical-intertropical difference driven by tropical convection and subtropical subsidence, and the northern hemispheric enhancement in spring and summer due to photochemistry. Comparison to ozonesondes in Fig. 7 allows us to extend the evaluation to high northern high

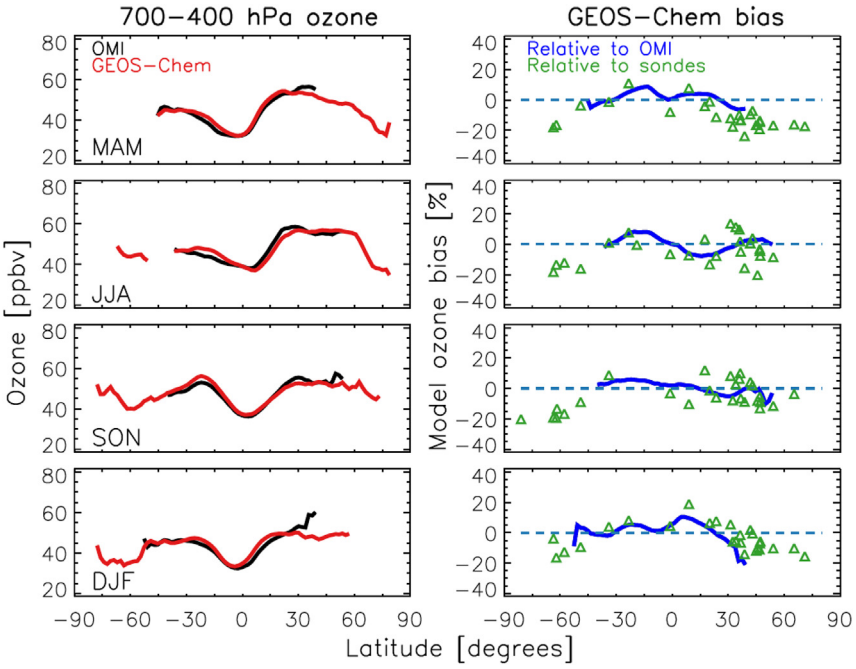

Fig. 7. Mean latitudinal variation of 700–400 hPa ozone in June 2012–May 2013. The left panel shows zonally averaged OMI observations, corrected for the global mean positive bias of 3.6 ppbv relative to ozonesondes, and the GEOS-Chem simulation sampled along the OMI orbit tracks and with averaging kernels applied. OMI data poleward of 45° in winter-spring are excluded because of large errors relative to ozonesondes (Fig. 4). The right panel shows the zonally averaged model differences at 700-400 hPa relative to OMI (blue solid line; difference between the two curves on the left panel) and the local differences relative to ozonesonde sites (green triangles; each triangle represents seasonal model biases for a given sonde launch site with at least 9 profiles per season). Positive values indicate model overestimates. (For interpretation of the references to colour in this figure legend, the reader is referred to the web version of this article.)

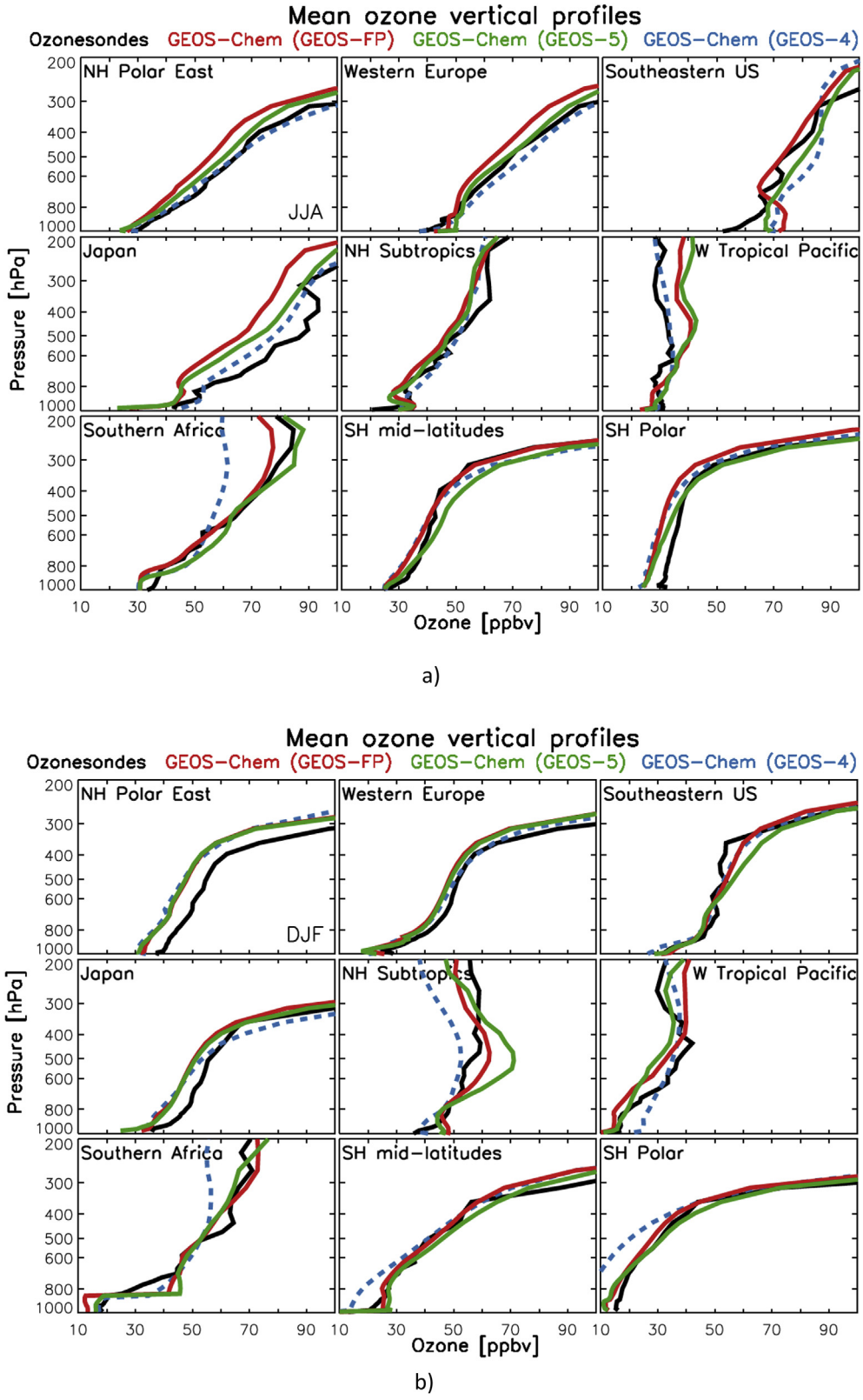

Fig. 8. a. Mean ozone vertical profiles for representative global regions in June–August 2012. Ozonesonde observations are averaged over the regions in Fig. 2. GEOS-Chem model output is sampled for the sonde launch time and locations, and is shown for the standard simulation driven by GEOS-FP meteorological fields and for sensitivity simulations driven by GEOS-5 fields and by by GEOS-4 fields (the latter for 2005 and sampled only for sonde locations). b. Same as Fig. 8a but for December–February 2012–2013.

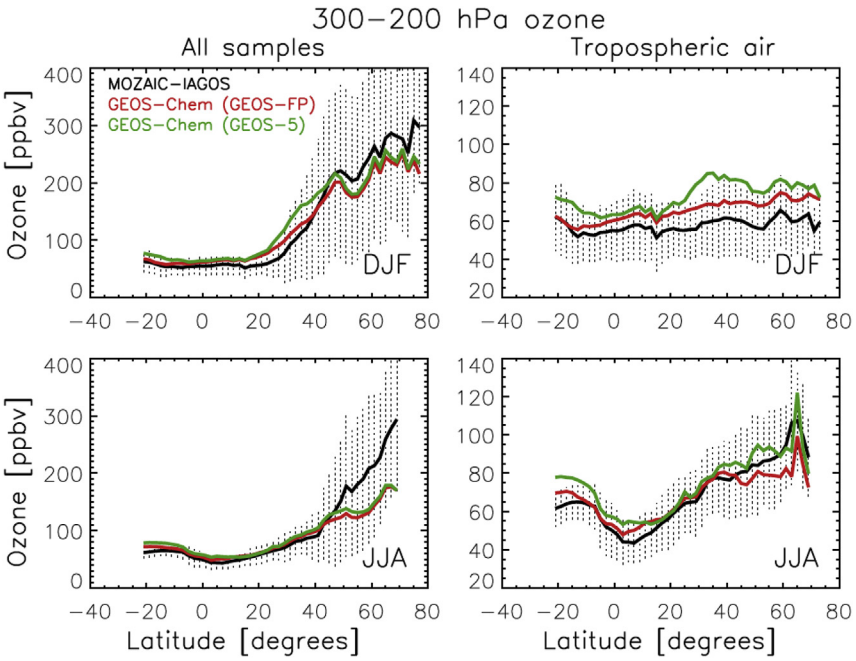

Fig. 9. Mean latitudinal distributions of ozone concentrations at 300-200 hPa along the cruise tracks of the MOZAIC-IAGOS aircraft in June 2012–May 2013 (Fig. 2). Observations are compared to GEOS-Chem model values sampled along the flight tracks, for the standard simulation using GEOS-FP meteorological data and a sensitivity simulation using GEOS-5 meteorological data. Stippling indicates standard deviations in the observations. The right panel excludes stratospheric conditions as diagnosed by either observed or simulated O_3/CO concentration ratios greater than 1.25 mol mol^{-1}.

latitudes where OMI data quality is poor. The ozonesonde data confirm the northern mid-latitudes model bias in winter-spring and show that it extends to the Arctic.

4.2. Evaluation with ozonesonde and MOZAIC-IAGOS aircraft observations

Fig. 8 provides further model evaluation of the ozone vertical distribution in comparison to the sonde data in DJF and JJA. Also shown are sensitivity simulations using different meteorological fields, GEOS-5 and GEOS-4 (the latter for 2005). Biases are generally less than 8 ppbv in the lower troposphere. Ozone is underestimated throughout the troposphere at high latitudes and in Western Europe in the standard GEOS-Chem simulation, but this bias is highly sensitive to meteorological fields and is largely absent in the simulation using GEOS-4 data. This may be due to differences in stratosphere-troposphere exchange (STE), as discussed below in the context of the global model budget. Large model biases over Japan are also very sensitive to the choice of meteorological fields. The lower tropospheric overestimate over the eastern US in summer is likely due to an overestimate of NO_x emissions in the US EPA inventory (Goldberg et al., 2016; Travis et al., 2016).

Fig. 9 compares the model to the MOZAIC-IAGOS commercial aircraft observations at 300-200 hPa. Comparison for the ensemble of data shows little model bias except for an underestimate north of 45°N in JJA. The extratropics at 300-200 hPa are variably in the troposphere or stratosphere, and this is reflected by the large standard deviations in the observations (Fig. 9). A small upward shift in the location of the tropopause would be enough to explain the model underestimate in JJA. Indeed, this shift is apparent in the ozonesonde profiles of Fig. 8. When stratospheric air is removed on the basis of $[O_3]/[CO] > 1.25$ mol mol^{-1} (either in the model or in the observations), the model can reproduce the large tropics-to-extratropics gradient in JJA when photochemical formation dominates (Fig. 9, right panel). In DJF, the model is too high at all latitudes.

5. Global budget of tropospheric ozone

The model evaluation presented here suggests that the v10-01 version of GEOS-Chem improves the simulation of global tropospheric ozone relative to earlier GEOS-Chem model versions. The previous evaluation of Zhang et al. (2010) using v8-01-04 found systematic underestimate of ozone in the tropics by ~10 ppbv and

Table 2
Global budget of tropospheric ozone in GEOS-Chem [a].

Sources, Tg a^{-1}	
Chemical production	4960
$HO_2 + NO$	66%
$CH_3O_2 + NO$	25%
$RO_2 + NO$ [b]	9%
Stratosphere-troposphere exchange [c]	325
Total	5290
Sinks, Tg a^{-1}	
Chemical loss	4360
$O(^1D) + H_2O$	51%
$HO_2 + O_3$	27%
$OH + O_3$	15%
$HOBr + h\nu$ [d]	4%
Others	3%
Dry deposition	908
Wet deposition [e]	17
Total	5290
Burden, Tg	351
Lifetime, d	24.2

[a] From the standard GEOS-Chem v10-01 simulation for 2012–2013 as described in the text. Budget is for the odd oxygen family $O_x \equiv O_3 + NO_2 + 2NO_3 + 3N_2O_5 + HNO_3 + HNO_4 + PANs + BrO + HOBr + BrNO_2 + 2BrNO_3$ to account for rapid cycling between O_x components. Ozone accounts for >95% of total O_x.

[b] $RO_2 \equiv$ organic peroxy radicals other than CH_3O_2.

[c] Inferred from the residual of mass balance between tropospheric chemical production, chemical loss, and deposition, verifying that the accumulation term ($d[O_3]/dt$) is negligibly small on a global annual basis.

[d] BrO/HOBr catalytic cycle (Parrella et al., 2012).

[e] Mainly as HNO_3.

Table 3
Global budgets of tropospheric ozone in the literature [a].

	Sources, Tg a^{-1}		Sinks, Tg a^{-1}		Burden, Tg	Lifetime, d
	Chemical production	Stratosphere-troposphere exchange	Chemical loss	Dry deposition		
IPCC TAR [b]	3420 ± 770	770 ± 400	3470 ± 520	770 ± 180	300 ± 30	24.0 ± 2.0
ACCENT [c]	4970 ± 220	560 ± 150	4570 ± 290	950 ± 150	336 ± 27	22.2 ± 2.2
GEOS-Chem v7-02-04 [d]	4470 ± 180	520 ± 15	3940 ± 175	1050 ± 45	310 ± 10	22.3 ± 0.9
ACCMIP [e]	4880 ± 850	480 ± 100	4260 ± 650	1090 ± 260	337 ± 23	23.4 ± 2.2
IPCC AR5 [f]	4620 ± 380	490 ± 90	4190 ± 380	960 ± 140	330 ± 17	N/A
GEOS-Chem v10-01 (this work) [g]	4960	325	4360	910	351	24.2

[a] Model intercomparisons, with standard deviations describing the spread between models. Entries are listed chronologically.
[b] Prather et al. (2001).
[c] Stevenson et al. (2006).
[d] Wu et al. (2007).
[e] Young et al. (2013).
[f] Myhre et al. (2013).
[g] From Table 2.

overestimate in the northern subtropics and at southern mid-latitudes by ~4–8 ppbv. A prominent flaw in the current version is the underestimate at high northern latitudes particularly in winter-spring. This may reflect insufficient STE, as discussed below.

Table 2 shows the global tropospheric ozone budget in GEOS-Chem v10-01 and the contributions from individual reactions. Table 3 compares to the budgets from several community intercomparisons. The global tropospheric chemical production of 4960 Tg a^{-1} is consistent with the current generation of models. The STE ozone flux in GEOS-Chem v10-01 is 325 Tg a^{-1}, lower than other models or the observational constraint of 550 ± 140 Tg a^{-1} (Gettelman et al., 1997; Olsen et al., 2001), although that constraint is for the downward flux at extratropical latitudes and would not include compensation for tropical upwelling. Older models reviewed in the IPCC TAR had much higher STE (770 ± 400 Tg a^{-1}) which may have been caused by errors in cross-tropopause transport.

We examined the sensitivity of the GEOS-Chem ozone budget to recent model developments including meteorological fields (Table 4). There is strong sensitivity to meteorological fields alone. The ozone production rate increases from 4960 Tg a^{-1} in the standard simulation driven by GEOS-FP to 5440 Tg a^{-1} in GEOS-5 and 5530 Tg a^{-1} in GEOS-4. At the same time, the ozone lifetime decreases from 24.2 days in GEOS-FP to 22.5 days in GEOS-5 and 20.9 days in GEOS-4. The difference is likely driven by deep convection frequency in the tropics (Liu J et al., 2010). GEOS-FP has much weaker subgrid parameterized convection than either GEOS-5 or GEOS-4, in part because of its higher horizontal resolution resolving convective motions on the grid scale, and this is not fully compensated by grid-scale vertical advection (Molod et al., 2015). Averaging native meteorological inputs to coarse resolution in GEOS-Chem further weakens vertical advection as eddy fluxes are averaged out (Yu et al., 2017). Deep convection decreases the ozone lifetime by bringing upper tropospheric ozone down to the lower troposphere where loss is fast (Lawrence et al., 2003). At the same time, deep convection injects NO_x to the upper troposphere where the ozone production efficiency is high (Pickering et al., 1990). A sensitivity simulation with no convection yields an ozone production rate of 4780 Tg a^{-1} and lifetime of 25.5 days (Table 4). Meteorological fields also affect the STE (325 Tg a^{-1} in GEOS-FP, 360 Tg a^{-1} in GEOS-5, 492 Tg a^{-1} in GEOS-4). The higher STE in GEOS-4 may reflect in part the strong deep convection in the tropics, resulting in low ozone in the tropical upper troposphere (Fig. 8) and hence a low tropical upwelling flux to compensate for the mid-latitudes downwelling flux.

6. Conclusions

Improvements in the GEOS-Chem chemical transport model over the past 10 years have led to a gradual increasing trend in the model-calculated tropospheric ozone burden and production rate. These improvements relate in particular to anthropogenic

Table 4
Global budget of tropospheric ozone in GEOS-Chem sensitivity simulations [a].

Simulations	GEOS-FP [b]	GEOS-5 [c]	GEOS-4 [d]	No convection [e]	Reduced emission [f]	No bromine [g]	Increased isoprene nitrates [h]
Sources, Tg a^{-1}							
Chemical production	4960	5440	5530	4780	4690	5080	4630
Stratosphere-troposphere exchange	325	360	492	314	353	304	337
Sinks, Tg a^{-1}							
Chemical loss	4360	4800	4960	4220	4170	4420	4090
Dry deposition	908	967	1040	864	860	943	856
Wet deposition	17	28	28	6	14	17	16
Burden, Tg	351	357	345	355	340	361	338
Lifetime, d	24.2	22.5	20.9	25.5	24.7	24.5	24.9

[a] Sensitivity simulations are relative to the base GEOS-Chem v10-01 simulation using GEOS-FP meteorological data as summarized in Table 2 and in the first column of this Table.
[b] Base simulation described in the text and Table 2 for 2012–2013.
[c] With GEOS-5 meteorological data.
[d] With GEOS-4 meteorological data for 2005.
[e] Without subgrid convective transport but with identical lightning as the base simulation.
[f] With global anthropogenic NO_x and CO emissions reduced by 30%.
[g] Without tropospheric bromine chemistry.
[h] With a higher yield of isoprene nitrates (18%) and no NOx recycling from these nitrates, as in Zhang et al. (2010).

emissions, lightning, bromine chemistry, isoprene chemistry, and driving meteorology. The increase in the tropospheric ozone budget continues a trend that was already apparent in pre-2006 versions of GEOS-Chem as reported by Wu et al. (2007). Here we present a thorough evaluation of the v10-01 standard version of GEOS-Chem for global tropospheric ozone in 2012–2013 using an ensemble of observations from ozonesondes, satellite (OMI), and aircraft (MOZAIC-IAGOS). We interpret the results in terms of their implication for the global budget of tropospheric ozone in GEOS-Chem and place the results in context of the literature.

OMI satellite data provide a particularly extensive data set for evaluation of mid-tropospheric ozone starting in 2005. There has been concern over instrument degradation starting in 2009. Here we validated the PROFOZ OMI 700-400 hPa retrieval for 2011–2013 with coincident ozonesondes. We find excellent agreement except at high latitudes in winter-spring. The global mean OMI bias relative to the sondes is 3.6 ± 8.5 ppbv for 2011–2013, as compared to 2.7 ± 6.6 ppbv for 2008 and previously reported 2.8 ± 6.6 ppbv for 2006. The bias has no apparent seasonal or latitudinal structure and can therefore be corrected as a uniform offset.

We find that the current GEOS-Chem simulation has no significant bias relative to the OMI 700-400 hPa ozone observations and high spatial correlation (R = 0.88–0.95 on a 2° × 2.5° grid). It improves on previous versions of GEOS-Chem (Zhang et al., 2010). The most pronounced flaw in the current version is an underestimate at high northern latitudes revealed by comparison to ozonesondes and MOZAIC-IAGOS data. This may reflect an underestimate of stratosphere-troposphere exchange (STE).

Tropospheric ozone in GEOS-Chem driven by the current-generation NASA GMAO GEOS-FP meteorological data has a global burden of 351 Tg, a global production rate of 4960 Tg a^{-1}, and a lifetime of 24.2 days. These values are on the high side of other models and higher than older versions of GEOS-Chem. Upward revisions of anthropogenic emissions in East Asia and improved isoprene nitrate chemistry have played a major role in increasing ozone production in GEOS-Chem. The ozone lifetime is sensitive to the intensity of deep tropical convection, and is shorter (20.9 days) when the same GEOS-Chem version uses older-generation GEOS-4 meteorological fields where convection is much stronger. We find that the STE is strongly anticorrelated to tropospheric ozone lifetime, implying that upward transport across the tropical tropopause may offset some of the stratospheric influx at extratropical latitudes.

Significant changes to the model tropospheric ozone budget may be expected in the near future with updates to tropospheric halogen chemistry. Bromine chemistry in the current standard GEOS-Chem simulation is from Parrella et al. (2012), but an improved representation of chlorine-bromine-iodine chemistry with better match to halogen radical observations has been developed recently for GEOS-Chem by Schmidt et al. (2016) and Sherwen et al. (2016a, 2016b). This causes further depletion of tropospheric ozone, particularly at high latitudes. On the other hand, STE in the current version of GEOS-Chem appears to be underestimated. Additional perturbations to the ozone budget may arise from updates to ozone deposition (Clifton et al., 2017; Luhar et al., 2017) and to NO_x chemistry (Ye et al., 2016; Reed et al., 2017). The ability of models to simulate long-term ozone trends must also be revisited (Young et al., in review). Better understanding of tropospheric ozone is likely to remain an important topic for research in the decade to come.

Acknowledgments

This work was supported by the NASA Atmospheric Composition Modeling and Analysis Program (ACMAP) and by the Atmospheric Chemistry Program of the National Science Foundation. MOZAIC/CARIBIC/IAGOS data were created with support from the European Commission, national agencies in Germany (BMBF), France (MESR), and the UK (NERC), and the IAGOS member institutions (http://www.iagos.org/partners). The participating airlines (Lufthansa, Air France, Austrian, China Airlines, Iberia, Cathay Pacific, Air Namibia, Sabena) supported IAGOS by carrying the measurement equipment free of charge since 1994. The data are available at http://www.iagos.fr thanks to additional support from AERIS. We also acknowledge all contributors to the ozonesonde data achieved at World Ozone and Ultraviolet Radiation Data Centre (WOUDC) website http://www.woudc.org.

Appendix A. Supplementary data

Supplementary data related to this article can be found at http://dx.doi.org/10.1016/j.atmosenv.2017.08.036.

References

Auvray, M., Bey, I., 2005. Long-range transport to Europe: seasonal variations and implications for the European ozone budget. J. Geophys. Res. Atmos. 110 (D11) http://dx.doi.org/10.1029/2004JD005503 n/a-n/a.

Bey, I., Jacob, D.J., Yantosca, R.M., Logan, J.A., Field, B.D., Fiore, A.M., Li, Q., Liu, H.Y., Mickley, L.J., Schultz, M.G., 2001. Global modeling of tropospheric chemistry with assimilated meteorology: model description and evaluation. J. Geophys. Res. 106 (D19), 23073–23095. http://dx.doi.org/10.1029/2001JD000807.

Bian, H., Prather, M.J., 2002. Fast-J2: accurate simulation of stratospheric photolysis in global chemical models. J. Atmos. Chem. 41 (3), 281–296. http://dx.doi.org/10.1023/a:1014980619462.

Brenninkmeijer, C.A.M., Crutzen, P., Boumard, F., Dauer, T., Dix, B., Ebinghaus, R., Filippi, D., Fischer, H., Franke, H., Frieβ, U., Heintzenberg, J., Helleis, F., Hermann, M., Kock, H.H., Koeppel, C., Lelieveld, J., Leuenberger, M., Martinsson, B.G., Miemczyk, S., Moret, H.P., Nguyen, H.N., Nyfeler, P., Oram, D., O'Sullivan, D., Penkett, S., Platt, U., Pupek, M., Ramonet, M., Randa, B., Reichelt, M., Rhee, T.S., Rohwer, J., Rosenfeld, K., Scharffe, D., Schlager, H., Schumann, U., Slemr, F., Sprung, D., Stock, P., Thaler, R., Valentino, F., van Velthoven, P., Waibel, A., Wandel, A., Waschitschek, K., Wiedensohler, A., Xueref-Remy, I., Zahn, A., Zech, U., Ziereis, H., 2007. Civil Aircraft for the regular investigation of the atmosphere based on an instrumented container: the new CARIBIC system. Atmos. Chem. Phys. 7 (18), 4953–4976. http://dx.doi.org/10.5194/acp-7-4953-2007.

Clifton, O.E., Fiore, A.M., Munger, J.W., Malyshev, S., Horowitz, L.W., Shevliakova, E., Paulot, F., Murray, L.T., Griffin, K.L., 2017. Interannual variability in ozone removal by a temperate deciduous forest. Geophys. Res. Lett. 44 (1) http://dx.doi.org/10.1002/2016GL070923, 2016GL070923.

Crounse, J.D., Paulot, F., Kjaergaard, H.G., Wennberg, P.O., 2011. Peroxy radical isomerization in the oxidation of isoprene. Phys. Chem. Chem. Phys. 13 (30), 13607–13613. http://dx.doi.org/10.1039/c1cp21330j.

Eastham, S.D., Weisenstein, D.K., Barrett, S.R.H., 2014. Development and evaluation of the unified tropospheric–stratospheric chemistry extension (UCX) for the global chemistry-transport model GEOS-Chem. Atmos. Environ. 89, 52–63. http://dx.doi.org/10.1016/j.atmosenv.2014.02.001.

Fiore, A.M., Dentener, F.J., Wild, O., Cuvelier, C., Schultz, M.G., Hess, P., Textor, C., Schulz, M., Doherty, R.M., Horowitz, L.W., MacKenzie, I.A., Sanderson, M.G., Shindell, D.T., Stevenson, D.S., Szopa, S., Van Dingenen, R., Zeng, G., Atherton, C., Bergmann, D., Bey, I., Carmichael, G., Collins, W.J., Duncan, B.N., Faluvegi, G., Folberth, G., Gauss, M., Gong, S., Hauglustaine, D., Holloway, T., Isaksen, I.S.A., Jacob, D.J., Jonson, J.E., Kaminski, J.W., Keating, T.J., Lupu, A., Marmer, E., Montanaro, V., Park, R.J., Pitari, G., Pringle, K.J., Pyle, J.A., Schroeder, S., Vivanco, M.G., Wind, P., Wojcik, G., Wu, S., Zuber, A., 2009. Multimodel estimates of intercontinental source-receptor relationships for ozone pollution. J. Geophys. Res. Atmos. 114 (D4), D04301. http://dx.doi.org/10.1029/2008JD010816.

Fishman, J., Larsen, J.C., 1987. Distribution of total ozone and stratospheric ozone in the tropics: implications for the distribution of tropospheric ozone. J. Geophys. Res. Atmos. 92 (D6), 6627–6634. http://dx.doi.org/10.1029/JD092iD06p06627.

Fishman, J., Minnis, P., Reichle, H.G., 1986. Use of satellite data to study tropospheric ozone in the tropics. J. Geophys. Res. Atmos. 91 (D13), 14451–14465. http://dx.doi.org/10.1029/JD091iD13p14451.

Gettelman, A., Holton, J.R., Rosenlof, K.H., 1997. Mass fluxes of O3, CH4, N2O and CF2Cl2 in the lower stratosphere calculated from observational data. J. Geophys. Res. Atmos. 102 (D15), 19149–19159. http://dx.doi.org/10.1029/97JD01014.

Giglio, L., Randerson, J.T., van der Werf, G.R., 2013. Analysis of daily, monthly, and annual burned area using the fourth-generation global fire emissions database (GFED4). J. Geophys. Res. Biogeosciences 118 (1), 317–328. http://dx.doi.org/10.1002/jgrg.20042.

Goldberg, D.L., Vinciguerra, T.P., Anderson, D.C., Hembeck, L., Canty, T.P., Ehrman, S.H., Martins, D.K., Stauffer, R.M., Thompson, A.M., Salawitch, R.J.,

Dickerson, R.R., 2016. CAMx ozone source attribution in the eastern United States using guidance from observations during DISCOVER-AQ Maryland. Geophys. Res. Lett. 43 (5), 2249–2258. http://dx.doi.org/10.1002/2015GL067332.

Guenther, A.B., Jiang, X., Heald, C.L., Sakulyanontvittaya, T., Duhl, T., Emmons, L.K., Wang, X., 2012. The Model of Emissions of Gases and Aerosols from Nature version 2.1 (MEGAN2.1): an extended and updated framework for modeling biogenic emissions. Geosci. Model Dev. 5, 1471–1492. http://dx.doi.org/10.5194/gmd-5-1471-2012.

Heikes, B.G., Chang, W.N., Pilson, M.E.Q., Swift, E., Singh, H.B., Guenther, A., Jacob, D.J., Field, B.D., Fall, R., Riemer, D., Brand, L., 2002. Atmospheric methanol budget and ocean implication. Glob. Biogeochem. Cy. 16 (4), 1133. http://dx.doi.org/10.1029/2002gb001895.

Hu, L., Millet, D.B., Baasandorj, M., Griffis, T.J., Turner, P., Helmig, D., Curtis, A.J., Hueber, J., 2015. Isoprene emissions and impacts over an ecological transition region in the U.S. Upper Midwest inferred from tall tower measurements. J. Geophys. Res. 120, 3553–3571. http://dx.doi.org/10.1002/2014JD022732.

Huang, G., Liu, X., Chance, K., Yang, K., Bhartia, P.K., Cai, Z., Allaart, M., Ancellet, G., Calpini, B., Coetzee, G.J.R., Cuevas-Agulló, E., Cupeiro, M., De Backer, H., Dubey, M.K., Fuelberg, H.E., Fujiwara, M., Godin-Beekmann, S., Hall, T.J., Johnson, B., Joseph, E., Kivi, R., Kois, B., Komala, N., König-Langlo, G., Laneve, G., Leblanc, T., Marchand, M., Minschwaner, K.R., Morris, G., Newchurch, M.J., Ogino, S.Y., Ohkawara, N., Piters, A.J.M., Posny, F., Querel, R., Scheele, R., Schmidlin, F.J., Schnell, R.C., Schrems, O., Selkirk, H., Shiotani, M., Skrivánková, P., Stübi, R., Taha, G., Tarasick, D.W., Thompson, A.M., Thouret, V., Tully, M.B., Van Malderen, R., Vömel, H., von der Gathen, P., Witte, J.C., Yela, M., 2017. Validation of 10-year SAO OMI Ozone Profile (PROFOZ) product using ozonesonde observations. Atmos. Meas. Tech. 10 (7), 2455–2475. http://dx.doi.org/10.5194/amt-10-2455-2017.

Hudman, R.C., Moore, N.E., Mebust, A.K., Martin, R.V., Russell, A.R., Valin, L.C., Cohen, R.C., 2012. Steps towards a mechanistic model of global soil nitric oxide emissions: implementation and space based-constraints. Atmos. Chem. Phys. 12 (16), 7779–7795. http://dx.doi.org/10.5194/acp-12-7779-2012.

IUPAC, 2013. Task Group on Atmospheric Chemical Kinetic Data Evaluation by International Union of Pure and Applied Chemistry (IUPAC).

Jiang, Z., Worden, J.R., Jones, D.B.A., Lin, J.T., Verstraeten, W.W., Henze, D.K., 2015. Constraints on asian ozone using Aura TES, OMI and terra MOPITT. Atmos. Chem. Phys. 15 (1), 99–112. http://dx.doi.org/10.5194/acp-15-99-2015.

Johnson, M., Kuang, S., Wang, L., Newchurch, M., 2016. Evaluating summer-time ozone enhancement events in the Southeast United States. Atmosphere 7 (8), 108.

Karl, T., Harley, P., Emmons, L., Thornton, B., Guenther, A., Basu, C., Turnipseed, A., Jardine, K., 2010. Efficient atmospheric cleansing of oxidized organic trace gases by vegetation. Science 330 (6005), 816–819. http://dx.doi.org/10.1126/science.1192534.

Keller, C.A., Long, M.S., Yantosca, R.M., Da Silva, A.M., Pawson, S., Jacob, D.J., 2014. HEMCO v1.0: a versatile, ESMF-compliant component for calculating emissions in atmospheric models. Geosci. Model Dev. 7 (4), 1409–1417. http://dx.doi.org/10.5194/gmd-7-1409-2014.

Kim, P.S., Jacob, D.J., Liu, X., Warner, J.X., Yang, K., Chance, K., Thouret, V., Nedelec, P., 2013. Global ozone–CO correlations from OMI and AIRS: constraints on tropospheric ozone sources. Atmos. Chem. Phys. 13 (18), 9321–9335. http://dx.doi.org/10.5194/acp-13-9321-2013.

Kuhns, H., Knipping, E.M., Vukovich, J.M., 2005. Development of a United States–Mexico emissions inventory for the big bend regional aerosol and visibility observational (BRAVO) study. J. Air Waste Manage. Assoc. 55 (5), 677–692. http://dx.doi.org/10.1080/10473289.2005.10464648.

Lawrence, M.G., von Kuhlmann, R., Salzmann, M., Rasch, P.J., 2003. The balance of effects of deep convective mixing on tropospheric ozone. Geophys. Res. Lett. 30 (18), 1940. http://dx.doi.org/10.1029/2003GL017644.

Li, M., Zhang, Q., Streets, D.G., He, K.B., Cheng, Y.F., Emmons, L.K., Huo, H., Kang, S.C., Lu, Z., Shao, M., Su, H., Yu, X., Zhang, Y., 2014. Mapping Asian anthropogenic emissions of non-methane volatile organic compounds to multiple chemical mechanisms. Atmos. Chem. Phys. 14 (11), 5617–5638. http://dx.doi.org/10.5194/acp-14-5617-2014.

Liu, X., Chance, K., Sioris, C.E., Spurr, R.J.D., Kurosu, T.P., Martin, R.V., Newchurch, M.J., 2005. Ozone profile and tropospheric ozone retrievals from the Global Ozone Monitoring Experiment: algorithm description and validation. J. Geophys. Res. Atmos. 110 (D20), D20307,. http://dx.doi.org/10.1029/2005JD006240.

Liu, X., Chance, K., Sioris, C.E., Kurosu, T.P., Spurr, R.J.D., Martin, R.V., Fu, T.-M., Logan, J.A., Jacob, D.J., Palmer, P.I., Newchurch, M.J., Megretskaia, I.A., Chatfield, R.B., 2006. First directly retrieved global distribution of tropospheric column ozone from GOME: comparison with the GEOS-CHEM model. J. Geophys. Res. Atmos. 111 (D2), D02308. http://dx.doi.org/10.1029/2005JD006564.

Liu, J., Logan, J.A., Jones, D.B.A., Livesey, N.J., Megretskaia, I., Carouge, C., Nedelec, P., 2010. Analysis of CO in the tropical troposphere using Aura satellite data and the GEOS-Chem model: insights into transport characteristics of the GEOS meteorological products. Atmos. Chem. Phys. 10 (24), 12207–12232. http://dx.doi.org/10.5194/acp-10-12207-2010.

Liu, X., Bhartia, P.K., Chance, K., Spurr, R.J.D., Kurosu, T.P., 2010. Ozone profile retrievals from the ozone monitoring instrument. Atmos. Chem. Phys. 10 (5), 2521–2537. http://dx.doi.org/10.5194/acp-10-2521-2010.

Logan, J.A., 1999. An analysis of ozonesonde data for the troposphere: recommendations for testing 3-D models and development of a gridded climatology for tropospheric ozone. J. Geophys. Res. Atmos. 104 (D13), 16115–16149. http://dx.doi.org/10.1029/1998JD100096.

Luhar, A.K., Galbally, I.E., Woodhouse, M.T., Thatcher, M., 2017. An improved parameterisation of ozone dry deposition to the ocean and its impact in a global climate–chemistry model. Atmos. Chem. Phys. 17 (5), 3749–3767. http://dx.doi.org/10.5194/acp-17-3749-2017.

Mao, J., Jacob, D.J., Evans, M.J., Olson, J.R., Ren, X., Brune, W.H., Clair, J.M.S., Crounse, J.D., Spencer, K.M., Beaver, M.R., Wennberg, P.O., Cubison, M.J., Jimenez, J.L., Fried, A., Weibring, P., Walega, J.G., Hall, S.R., Weinheimer, A.J., Cohen, R.C., Chen, G., Crawford, J.H., McNaughton, C., Clarke, A.D., Jaeglé, L., Fisher, J.A., Yantosca, R.M., Le Sager, P., Carouge, C., 2010. Chemistry of hydrogen oxide radicals (HO_x) in the Arctic troposphere in spring. Atmos. Chem. Phys. 10 (13), 5823–5838. http://dx.doi.org/10.5194/acp-10-5823-2010.

Mao, J., Paulot, F., Jacob, D.J., Cohen, R.C., Crounse, J.D., Wennberg, P.O., Keller, C.A., Hudman, R.C., Barkley, M.P., Horowitz, L.W., 2013. Ozone and organic nitrates over the eastern United States: sensitivity to isoprene chemistry. J. Geophys. Res. 118 (19) http://dx.doi.org/10.1002/jgrd.50817, 2013JD020231, doi: 020210.021002/jgrd.050817.

Marais, E.A., Jacob, D.J., Kurosu, T.P., Chance, K., Murphy, J.G., Reeves, C., Mills, G., Casadio, S., Millet, D.B., Barkley, M.P., Paulot, F., Mao, J., 2012. Isoprene emissions in Africa inferred from OMI observations of formaldehyde columns. Atmos. Chem. Phys. 12 (14), 6219–6235. http://dx.doi.org/10.5194/acp-12-6219-2012.

Martin, R.V., Sauvage, B., Folkins, I., Sioris, C.E., Boone, C., Bernath, P., Ziemke, J., 2007. Space-based constraints on the production of nitric oxide by lightning. J. Geophys. Res. Atmos. 112 (D9), D09309. http://dx.doi.org/10.1029/2006JD007831.

McLinden, C.A., Olsen, S.C., Hannegan, B., Wild, O., Prather, M.J., Sundet, J., 2000. Stratospheric ozone in 3-D models: a simple chemistry and the cross-tropopause flux. J. Geophys. Res. Atmos. 105 (D11), 14653–14665. http://dx.doi.org/10.1029/2000JD900124.

McPeters, R.D., Labow, G.J., Logan, J.A., 2007. Ozone climatological profiles for satellite retrieval algorithms. J. Geophys. Res. Atmos. 112 (D5), D05308. http://dx.doi.org/10.1029/2005JD006823.

Mickley, L.J., Jacob, D.J., Rind, D., 2001. Uncertainty in preindustrial abundance of tropospheric ozone: implications for radiative forcing calculations. J. Geophys. Res. Atmos. 106 (D4), 3389–3399. http://dx.doi.org/10.1029/2000JD900594.

Molod, A., Takacs, L., Suarez, M., Bacmeister, J., 2015. Development of the GEOS-5 atmospheric general circulation model: evolution from MERRA to MERRA2. Geosci. Model Dev. 8 (5), 1339–1356. http://dx.doi.org/10.5194/gmd-8-1339-2015.

Murray, L.T., Jacob, D.J., Logan, J.A., Hudman, R.C., Koshak, W.J., 2012. Optimized regional and interannual variability of lightning in a global chemical transport model constrained by LIS/OTD satellite data. J. Geophys. Res. Atmos. 117 (D20), D20307. http://dx.doi.org/10.1029/2012JD017934.

Myhre, G., Shindell, D., Breon, F.-M., Collins, W., Fuglestvedt, J., Huang, J., Koch, D., Lamarque, J.-F., Lee, D., Mendoza, B., Nakajima, T., Robock, A., Stephens, G., Takemura, T., Zhang, H., 2013. Anthropogenic and natural radiative forcing. Contribution of Working Group I to the Fifth Assessment Report of the Intergovernmental Panel on Climate Change. In: Stocker, T.F., Qin, D., Plattner, G.-K., Tignor, M., Allen, S.K., Boschung, J., Nauels, A., Xia, Y., Bex, V., Midgley, P.M. (Eds.), Climate Change 2013: the Physical Science Basis. Cambridge University Press, Cambridge, United Kingdom and New York, NY, USA, pp. 659–740. http://dx.doi.org/10.1017/CBO9781107415324.018.

Nedelec, P., Cammas, J.P., Thouret, V., Athier, G., Cousin, J.M., Legrand, C., Abonnel, C., Lecoeur, F., Cayez, G., Marizy, C., 2003. An improved infrared carbon monoxide analyser for routine measurements aboard commercial Airbus aircraft: technical validation and first scientific results of the MOZAIC III programme. Atmos. Chem. Phys. 3 (5), 1551–1564. http://dx.doi.org/10.5194/acp-3-1551-2003.

Nédélec, P., Blot, R., Boulanger, D., Athier, G., Cousin, J.-M., Gautron, B., Petzold, A., Volz-Thomas, A., Thouret, V., 2015, 2015. Instrumentation on Commercial Aircraft for Monitoring the Atmospheric Composition on a Global Scale: the IAGOS System, Technical Overview of Ozone and Carbon Monoxide Measurements, vol. 67. http://dx.doi.org/10.3402/tellusb.v67.27791.

Olivier, J.G.J., Berdowski, J.J.M., 2001. Global emission sources and sinks. In: Berdowski, J., Guicherit, R., Heij, B.J. (Eds.), The Climate System. A.A. Balkema Publishers/Swets & Zeitlinger Publishers, Lisse, The Netherlands, pp. 33–78.

Olsen, S.C., McLinden, C.A., Prather, M.J., 2001. Stratospheric N2O–NO y system: testing uncertainties in a three-dimensional framework. J. Geophys. Res. Atmos. 106 (D22), 28771–28784. http://dx.doi.org/10.1029/2001JD000559.

Ott, L.E., Pickering, K.E., Stenchikov, G.L., Allen, D.J., DeCaria, A.J., Ridley, B., Lin, R.-F., Lang, S., Tao, W.-K., 2010. Production of lightning NOx and its vertical distribution calculated from three-dimensional cloud-scale chemical transport model simulations. J. Geophys. Res. Atmos. 115 (D4) http://dx.doi.org/10.1029/2009JD011880 n/a-n/a.

Parrella, J.P., Jacob, D.J., Liang, Q., Zhang, Y., Mickley, L.J., Miller, B., Evans, M.J., Yang, X., Pyle, J.A., Theys, N., Van Roozendael, M., 2012. Tropospheric bromine chemistry: implications for present and pre-industrial ozone and mercury. Atmos. Chem. Phys. 12 (15), 6723–6740. http://dx.doi.org/10.5194/acp-12-6723-2012.

Parrish, D.D., Lamarque, J.F., Naik, V., Horowitz, L., Shindell, D.T., Staehelin, J., Derwent, R., Cooper, O.R., Tanimoto, H., Volz-Thomas, A., Gilge, S., Scheel, H.E., Steinbacher, M., Fröhlich, M., 2014. Long-term changes in lower tropospheric baseline ozone concentrations: comparing chemistry-climate models and observations at northern midlatitudes. J. Geophys. Res. Atmos. 119 (9) http://dx.doi.org/10.1002/2013JD021435, 2013JD021435.

Paulot, F., Crounse, J.D., Kjaergaard, H.G., Kroll, J.H., Seinfeld, J.H., Wennberg, P.O., 2009a. Isoprene photooxidation: new insights into the production of acids and organic nitrates. Atmos. Chem. Phys. 9 (4), 1479–1501. http://dx.doi.org/10.5194/acp-9-1479-2009.

Paulot, F., Crounse, J.D., Kjaergaard, H.G., Kürten, A., St Clair, J.M., Seinfeld, J.H., Wennberg, P.O., 2009b. Unexpected epoxide formation in the gas-phase photooxidation of isoprene. Science 325 (5941), 730–733. http://dx.doi.org/10.1126/science.1172910.

Philip, S., Martin, R.V., Keller, C.A., 2016. Sensitivity of chemistry-transport model simulations to the duration of chemical and transport operators: a case study with GEOS-Chem v10-01. Geosci. Model Dev. 9 (5), 1683–1695. http://dx.doi.org/10.5194/gmd-9-1683-2016.

Pickering, K.E., Thompson, A.M., Dickerson, R.R., Luke, W.T., McNamara, D.P., Greenberg, J.P., Zimmerman, P.R., 1990. Model calculations of tropospheric ozone production potential following observed convective events. J. Geophys. Res. Atmos. 95 (D9), 14049–14062. http://dx.doi.org/10.1029/JD095iD09p14049.

Prather, M., Ehhalt, D., Dentener, F., Derwent, R., Dlugokencky, E., Holland, E., Isaksen, I., Katima, J., Kirchhoff, V., Matson, P., 2001. Atmospheric chemistry and greenhouse gases. In: Climate Change 2001: the Scientific Basis—contribution of Working Group I to the Third Assessment Report of the Intergovernmental Panel on Climate Change. Cambridge Univ. Press, New York.

Reed, C., Evans, M.J., Crilley, L.R., Bloss, W.J., Sherwen, T., Read, K.A., Lee, J.D., Carpenter, L.J., 2017. Evidence for renoxification in the tropical marine boundary layer. Atmos. Chem. Phys. 17 (6), 4081–4092. http://dx.doi.org/10.5194/acp-17-4081-2017.

Sander, S.P., Golden, D., Kurylo, M., Moortgat, G., Wine, P., Ravishankara, A., Kolb, C., Molina, M., Finlayson-Pitts, B., Huie, R., 2011. Chemical kinetics and photochemical data for use in atmospheric studies. JPL Publ. 06–2, 684.

Sauvage, B., Martin, R.V., van Donkelaar, A., Liu, X., Chance, K., Jaeglé, L., Palmer, P.I., Wu, S., Fu, T.M., 2007. Remote sensed and in situ constraints on processes affecting tropical tropospheric ozone. Atmos. Chem. Phys. 7 (3), 815–838. http://dx.doi.org/10.5194/acp-7-815-2007.

Schmidt, J.A., Jacob, D.J., Horowitz, H.M., Hu, L., Sherwen, T., Evans, M.J., Liang, Q., Suleiman, R.M., Oram, D.E., Le Breton, M., Percival, C.J., Wang, S., Dix, B., Volkamer, R., 2016. Modeling the observed tropospheric BrO background: importance of multiphase chemistry and implications for ozone, OH, and mercury. J. Geophys. Res. Atmos. http://dx.doi.org/10.1002/2015JD024229, 2015JD024229.

Schultz, M., Backman, L., Balkanski, Y., Bjoerndalsaeter, S., Brand, R., Burrows, J., Dalsoeren, S., de Vasconcelos, M., Grodtmann, B., Hauglustaine, D., 2007. REanalysis of the TROpospheric Chemical Composition over the Past 40 Years (RETRO) - a Long-term Global Modeling Study of Tropospheric Chemistry: Final Report. Jülich/Hamburg, Germany.

Schumann, U., Huntrieser, H., 2007. The global lightning-induced nitrogen oxides source. Atmos. Chem. Phys. 7 (14), 3823–3907. http://dx.doi.org/10.5194/acp-7-3823-2007.

Sherwen, T., Evans, M.J., Carpenter, L.J., Andrews, S.J., Lidster, R.T., Dix, B., Koenig, T.K., Sinreich, R., Ortega, I., Volkamer, R., Saiz-Lopez, A., Prados-Roman, C., Mahajan, A.S., Ordóñez, C., 2016a. Iodine's impact on tropospheric oxidants: a global model study in GEOS-Chem. Atmos. Chem. Phys. 16 (2), 1161–1186. http://dx.doi.org/10.5194/acp-16-1161-2016.

Sherwen, T., Schmidt, J.A., Evans, M.J., Carpenter, L.J., Großmann, K., Eastham, S.D., Jacob, D.J., Dix, B., Koenig, T.K., Sinreich, R., Ortega, I., Volkamer, R., Saiz-Lopez, A., Prados-Roman, C., Mahajan, A.S., Ordóñez, C., 2016b. Global impacts of tropospheric halogens (Cl, Br, I) on oxidants and composition in GEOS-Chem. Atmos. Chem. Phys. 16 (18), 12239–12271. http://dx.doi.org/10.5194/acp-16-12239-2016.

Sofen, E.D., Bowdalo, D., Evans, M.J., Apadula, F., Bonasoni, P., Cupeiro, M., Ellul, R., Galbally, I.E., Girgzdiene, R., Luppo, S., Mimouni, M., Nahas, A.C., Saliba, M., Tørseth, K., 2016. Gridded global surface ozone metrics for atmospheric chemistry model evaluation. Earth Syst. Sci. Data 8 (1), 41–59. http://dx.doi.org/10.5194/essd-8-41-2016.

Stettler, M.E.J., Eastham, S., Barrett, S.R.H., 2011. Air quality and public health impacts of UK airports. Part I Emiss. Atmos. Environ. 45 (31), 5415–5424. http://dx.doi.org/10.1016/j.atmosenv.2011.07.012.

Stevenson, D.S., Dentener, F.J., Schultz, M.G., Ellingsen, K., van Noije, T.P.C., Wild, O., Zeng, G., Amann, M., Atherton, C.S., Bell, N., Bergmann, D.J., Bey, I., Butler, T., Cofala, J., Collins, W.J., Derwent, R.G., Doherty, R.M., Drevet, J., Eskes, H.J., Fiore, A.M., Gauss, M., Hauglustaine, D.A., Horowitz, L.W., Isaksen, I.S.A., Krol, M.C., Lamarque, J.F., Lawrence, M.G., Montanaro, V., Müller, J.F., Pitari, G., Prather, M.J., Pyle, J.A., Rast, S., Rodriguez, J.M., Sanderson, M.G., Savage, N.H., Shindell, D.T., Strahan, S.E., Sudo, K., Szopa, S., 2006. Multimodel ensemble simulations of present-day and near-future tropospheric ozone. J. Geophys. Res. Atmos. 111 (D8), D08301. http://dx.doi.org/10.1029/2005JD006338.

Tanimoto, H., Zbinden, R.M., Thouret, V., Nédélec, P., 2015. Consistency of tropospheric ozone observations made by different platforms and techniques in the global databases. Tellus B 67. http://dx.doi.org/10.3402/tellusb.v67.27073.

Thompson, A.M., Witte, J.C., Smit, H.G.J., Oltmans, S.J., Johnson, B.J., Kirchhoff, V.W.J.H., Schmidlin, F.J., 2007. Southern Hemisphere Additional Ozonesondes (SHADOZ) 1998–2004 tropical ozone climatology: 3. Instrumentation, station-to-station variability, and evaluation with simulated flight profiles. J. Geophys. Res. Atmos. 112 (D3), D03304. http://dx.doi.org/10.1029/2005JD007042.

Thouret, V., Marenco, A., Nédélec, P., Grouhel, C., 1998. Ozone climatologies at 9–12 km altitude as seen by the MOZAIC airborne program between September 1994 and August 1996. J. Geophys. Res. Atmos. 103 (D19), 25653–25679. http://dx.doi.org/10.1029/98JD01807.

Tilmes, S., Lamarque, J.F., Emmons, L.K., Conley, A., Schultz, M.G., Saunois, M., Thouret, V., Thompson, A.M., Oltmans, S.J., Johnson, B., Tarasick, D., 2012. Technical Note: ozonesonde climatology between 1995 and 2011: description, evaluation and applications. Atmos. Chem. Phys. 12 (16), 7475–7497. http://dx.doi.org/10.5194/acp-12-7475-2012.

Travis, K.R., Jacob, D.J., Fisher, J.A., Kim, P.S., Marais, E.A., Zhu, L., Yu, K., Miller, C.C., Yantosca, R.M., Sulprizio, M.P., Thompson, A.M., Wennberg, P.O., Crounse, J.D., St Clair, J.M., Cohen, R.C., Laugher, J.L., Dibb, J.E., Hall, S.R., Ullmann, K., Wolfe, G.M., Pollack, I.B., Peischl, J., Neuman, J.A., Zhou, X., 2016. Why do models overestimate surface ozone in the Southeast United States? Atmos. Chem. Phys. 16, 13561–13577. http://dx.doi.org/10.5194/acp-16-13561-2016.

van Donkelaar, A., Martin, R.V., Leaitch, W.R., Macdonald, A.M., Walker, T.W., Streets, D.G., Zhang, Q., Dunlea, E.J., Jimenez, J.L., Dibb, J.E., Huey, L.G., Weber, R., Andreae, M.O., 2008. Analysis of aircraft and satellite measurements from the Intercontinental Chemical Transport Experiment (INTEX-B) to quantify long-range transport of East Asian sulfur to Canada. Atmos. Chem. Phys. 8 (11), 2999–3014. http://dx.doi.org/10.5194/acp-8-2999-2008.

Volz-Thomas, A., Cammas, J.-P., Brenninkmeijer, C.A.M., Machida, T., Cooper, O., Sweeney, C., Waibel, A., 2009. Civil Aviation Monitors Air Quality and Climate, Em Magazine, Air & Waste Management Association. October, 16–19.

Wang, Y., Jacob, D.J., Logan, J.A., 1998. Global simulation of tropospheric O3-NO x -hydrocarbon chemistry: 3. Origin of tropospheric ozone and effects of non-methane hydrocarbons. J. Geophys. Res. Atmos. 103 (D9), 10757–10767. http://dx.doi.org/10.1029/98JD00156.

Wang, Y., Zhang, Y., Hao, J., Luo, M., 2011. Seasonal and spatial variability of surface ozone over China: contributions from background and domestic pollution. Atmos. Chem. Phys. 11 (7), 3511–3525. http://dx.doi.org/10.5194/acp-11-3511-2011.

Wesely, M.L., 1989. Parameterization of surface resistances to gaseous dry deposition in regional-scale numerical models. Atmos. Environ. 23 (6), 1293–1304.

Wild, O., 2007. Modelling the global tropospheric ozone budget: exploring the variability in current models. Atmos. Chem. Phys. 7 (10), 2643–2660. http://dx.doi.org/10.5194/acp-7-2643-2007.

Worden, H.M., Logan, J.A., Worden, J.R., Beer, R., Bowman, K., Clough, S.A., Eldering, A., Fisher, B.M., Gunson, M.R., Herman, R.L., Kulawik, S.S., Lampel, M.C., Luo, M., Megretskaia, I.A., Osterman, G.B., Shephard, M.W., 2007. Comparisons of Tropospheric Emission Spectrometer (TES) ozone profiles to ozonesondes: methods and initial results. J. Geophys. Res. Atmos. 112 (D3), D03309. http://dx.doi.org/10.1029/2006JD007258.

WOUDC, edited, WMO/GAW Ozone Monitoring Community, World Meteorological Organization-Global Atmosphere Watch Program (WMO-GAW)/World Ozone and Ultraviolet Radiation Data Centre (WOUDC). A list of all contributors is available on the website., doi:10.14287/10000001.

Wu, S., Mickley, L.J., Jacob, D.J., Logan, J.A., Yantosca, R.M., Rind, D., 2007. Why are there large differences between models in global budgets of tropospheric ozone? J. Geophys. Res. Atmos. 112 (D5), D05302. http://dx.doi.org/10.1029/2006JD007801.

Yan, Y., Lin, J., Chen, J., Hu, L., 2016. Improved simulation of tropospheric ozone by a global-multi-regional two-way coupling model system. Atmos. Chem. Phys. 16 (4), 2381–2400. http://dx.doi.org/10.5194/acp-16-2381-2016.

Ye, C., Zhou, X., Pu, D., Stutz, J., Festa, J., Spolaor, M., Tsai, C., Cantrell, C., Mauldin, R.L., Campos, T., Weinheimer, A., Hornbrook, R.S., Apel, E.C., Guenther, A., Kaser, L., Yuan, B., Karl, T., Haggerty, J., Hall, S., Ullmann, K., Smith, J.N., Ortega, J., Knote, C., 2016. Rapid cycling of reactive nitrogen in the marine boundary layer. Nature 532 (7600), 489–491. http://dx.doi.org/10.1038/nature17195.

Yevich, R., Logan, J.A., 2003. An assessment of biofuel use and burning of agricultural waste in the developing world. Glob. Biogeochem. Cycles 17 (4), 1095. http://dx.doi.org/10.1029/2002GB001952.

Young, P.J., Archibald, A.T., Bowman, K.W., Lamarque, J.F., Naik, V., Stevenson, D.S., Tilmes, S., Voulgarakis, A., Wild, O., Bergmann, D., Cameron-Smith, P., Cionni, I., Collins, W.J., Dalsøren, S.B., Doherty, R.M., Eyring, V., Faluvegi, G., Horowitz, L.W., Josse, B., Lee, Y.H., MacKenzie, I.A., Nagashima, T., Plummer, D.A., Righi, M., Rumbold, S.T., Skeie, R.B., Shindell, D.T., Strode, S.A., Sudo, K., Szopa, S., Zeng, G., 2013. Pre-industrial to end 21st century projections of tropospheric ozone from the atmospheric chemistry and climate model intercomparison project (ACCMIP). Atmos. Chem. Phys. 13 (4), 2063–2090. http://dx.doi.org/10.5194/acp-13-2063-2013.

Young P.J., Naik V., Fiore A.M., Gaudel A., Guo J., Lin M.Y., Neu J., Parrish D.D., Rieder H.E., Schnell J.L., Tilmes S., Wild O., Zhang L., Brandt J., Delcloo A., Doherty R.M., Geels C., Hegglin M.I., Hu L., Im U., Kumar R., Luhar A., Murray L., Plummer D., Rodriguez J., Saiz-Lopez A., Schultz M.G., Woodhouse M., Zeng G. and Ziemke J., Tropospheric Ozone Assessment Report: assessment of global-scale model performance for global and regional ozone distributions, variability, and trends, Elem. Sci. Anth. in review.

Yu, K., Keller, C.A., Jacob, D.J., Molod, A.M., Eastham, S.D., Long, M.S., 2017. Errors and improvements in the use of archived meteorological data for chemical transport modeling. Geosci. Model Dev. Discuss. 2017, 1–22. http://dx.doi.org/10.5194/gmd-2017-125.

Zhang, L., Jacob, D.J., Liu, X., Logan, J.A., Chance, K., Eldering, A., Bojkov, B.R., 2010. Intercomparison methods for satellite measurements of atmospheric composition: application to tropospheric ozone from TES and OMI. Atmos. Chem. Phys. 10 (10), 4725–4739. http://dx.doi.org/10.5194/acp-10-4725-2010.